ACS Catalysis

Research Article

pubs.acs.org/acscatalysis

Increasing *para*-Xylene Selectivity in Making Aromatics from Methanol with a Surface-Modified Zn/P/ZSM-5 Catalyst

Jingui Zhang, Weizhong Qian,* Chuiyan Kong, and Fei Wei

Department of Chemical Engineering, Tsinghua University, Beijing, 100084, China

Supporting Information

ABSTRACT: We report a ZSM-5 based catalyst with surface modification of SiO_2 to increase the selectivity of *para*-xylene (PX) in xylene (X) in the methanol-to-aromatics process. The effect of acid strength and acid amount in HZSM-5, Zn/P/ZSM-5, and Zn/P/Si/ZSM-5 on the catalytic performance, including methanol conversion, aromatic yield, and PX selectivity, were studied. The total acid strength and acid amount of the catalyst were crucial for high methanol conversion (around 100%) and high yield of aromatics (>60%), whereas weak external acid sites present in a small amount played an important role in increasing the PX selectivity (in the X isomers) from the usual 23−24% to 89.6%. The results validated the use of a catalyst having a core with strong acid sites in a large amount and an external shell with weak acid sites in a small amount. The contribution of the external surface reaction, including alkylation, isomerization, and dealkylation, to the PX selectivity was evaluated by using PX or *ortho*-X separately as feedstock. A Zn/P/Si/ZSM-5 catalyst worked well in continuous reaction/catalyst-regeneration cycles, and it also converted recycled toluene into PX by an alkylation route.

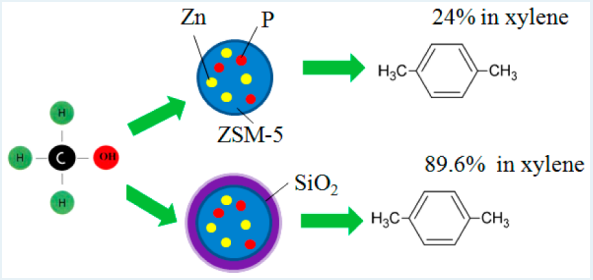

KEYWORDS: *methanol, aromatics, para-xylene, selectivity, ZSM-5 zeolite*

1. INTRODUCTION

The direct conversion of methanol over ZSM-5 zeolite produced a variety of hydrocarbons via the dual cycles of the aromatics carbon pool and olefins carbon pool.[1] The dope of metal on ZSM-5 improved the dehydrogenation activity of the catalyst and, consequently, increased the yield of aromatics.[2−13] As a result, the weight ratio of aromatics in liquid organic product in methanol to aromatics (MTA) process was around 90%, which is far higher than that in the methanol to gasoline (MTG; ∼35%) process and that in catalytic reforming of naphtha (50−65%).[1−13] In addition, the selectivity to *para*-xylene (PX) in xylene (X) in the MTA product is 23−24%, which is higher than that from the catalytic reforming of naphtha (around 18%). These features make the MTA product suitable for the production of pure PX. However, the transformation of a feedstock containing 23% PX in X into a pure PX product is still very energy-demanding. Increasing the selectivity of PX (in the following, the selectivity of PX refers to the proportion of PX in X) in the MTA process is important for making inexpensive PX and the consequent development of the polyethylene terephthalate industry, which has the capacity of several ten-million tons annually worldwide.

The formation of aromatics from methanol is a complicated process that includes the dehydration of methanol; formation of a hydrocarbon pool; and the production of aromatics and byproduct, including light olefins and paraffins.[1,2,7,13] As compared with the alkylation of toluene (T) with methanol, this process needs a catalyst with strong acidity to achieve a high yield of aromatics (60−70%) and high conversion of methanol (approaching 100%). However, side reactions, such as the alkylation of X, dealkylation of X, isomerization of X, and hydrogen transfer reactions, are simultaneously present with a zeolite catalyst. Among these, the isomerization of X results in a low selectivity to PX. Because isomerization is easily achieved by a catalyst with very weak acidity, as is known from other processes,[14−16] the suppression of the acidity of the catalyst is crucial to increasing the selectivity of PX,[14−21] but this suppression is in conflict with the general requirements of acid strength and acid amount of the MTA catalyst. It remains a challenge to design a multifunctional catalyst.

Here, we propose a ZSM-5-based catalyst with surface modification of SiO_2 designed to meet the above three requirements simultaneously. The core of the catalyst is Zn/P-doped ZSM-5 with a low Si/Al ratio (Zn/P/ZSM-5), which has a large amount of strong acid sites. The outer shell of the catalyst is a SiO_2 shell with weak acid sites prepared by a chemical liquid deposition (CLD) method.[22,23] We validated such a catalyst structure by varying the Si/Al ratio on the core of catalyst, the weight ratio of the SiO_2 shell of the catalyst, and the external acid amount on the PX selectity, methanol conversion, and aromatic yield. The contribution of the external surface reaction, including alkylation, isomerization, and dealkylation, to the selectivity of PX was quantitatively evaluated by using PX or *ortho*-X (OX) separately as feedstock.

Received: October 11, 2014
Revised: March 31, 2015
Published: April 7, 2015

DOI: 10.1021/acscatal.5b00192
ACS Catal. 2015, 5, 2982−2988

In addition, the Zn/P/Si/ZSM-5 catalyst can directly convert recycled T into PX with high selectivity by a reaction with methanol at the same operational condition as when the methanol was the feed. These results represented significant progress in the production of PX in high yield from methanol and in simplifying the downstream separation process.

2. EXPERIMENTAL SECTION

2.1. Catalyst Preparation. HZSM-5 zeolite (Si/Al of 12.5, 19, 25 and 40, Nankai University Catalyst Plant, China) was impregnated with $Zn(NO_3)_2$ solution and H_3PO_4 solution. The impregnated catalyst was dried at 110 °C for 12 h and then calcined in air at 600 °C for 4 h. The loading of Zn and P was 3% and 0.1%, respectively. The as-obtained catalyst was designated as Zn/P/ZSM-5. To get the Zn/P/Si/ZSM-5 catalyst, 10 g of Zn/P/ZSM-5 catalyst was suspended in 100 mL of hexane, then 20.83 g of tetraethylorthosilicate was added, and the mixture stirred for 4 h.[22] The sample was dried at 110 °C and calcined at 550 °C for 4 h. The loading of SiO_2 was 8 wt %. One cycle of CLD modification is effective to coat 5−8% SiO_2 on the Zn/P/ZSM-5. Two and three cycles were needed to coat 18% and 28% SiO_2 on the catalyst, respectively.

2.2. Catalyst Characterization. The morphology of Zn/P/ZSM-5 and Zn/P/Si/ZSM-5 was characterized by transmission electron microscope (TEM, JEOL-2010, 200 kV). The Si/Al ratios of the external surface and in the core of the different samples were measured by EDS. The crystallinity of the catalysts was characterized by X-ray diffraction (XRD, Bruker-800, Cu target). Raman characterization used a Horiba-800 instrument equipped with a 432 nm laser.

Ar adsorption at −186 °C (Quantachrome Instruments, Autosorb iQ) was used to measure the surface area and pore size distribution of the catalysts. The pore volume was determined by the NL-DFT method. The adsorption capacity of the catalyst was evaluated using PX or OX as adsorbent. PX or OX was fed using a saturator kept at 25 °C in a water bath. The carrier gas flow rate was 30 mL min^{-1} of nitrogen. The catalyst with adsorbed X was further characterized by thermogravimetric analysis (Mettler-Toledo TGA/DSC1 1600HT).

The acid strength and amount in the catalyst were measured by NH_3 temperature-programmed desorption (TPD, Quantachrome Instruments, Chembet PULSAR). The sample was first activated by heating at 600 °C for 1.5 h then cooled to 100 °C and kept in flowing NH_3 for 1 h. Physically adsorbed NH_3 was removed by flushing with He at 100 °C for 1 h, then the chemically adsorbed NH_3 on the catalyst was measured by heating from 100 to 800 °C with a heating rate of 10 °C min^{-1}. The amount of NH_3 adsorbed was monitored by a thermal conductivity detector. The amount of acid sites was then quantitatively determined by titration using ammonia pulses.

The type of acid sites on the catalyst was determined by IR spectroscopy (Nicolet Nexus 670 spectrometer) using the adsorption of pyridine. The catalyst sample was pressed into a self-supporting wafer and placed in a quartz holder with an attached heating filament. This was mounted in an in situ cell connected to a vacuum system. The sample was degassed in vacuum ($<10^{-4}$ Pa) by heating to 450 °C at a rate of 10 °C min^{-1} and held at this temperature for 4 h. After cooling to 100 °C, pyridine adsorption was performed by exposure to pyridine for 1 h, then the cell was evacuated to a pressure of 10^{-4} Pa. IR spectra were collected at 200 and 350 °C. For the quantitative comparison of the peak intensity, the IR spectra were normalized using the area of the overtone lattice vibration bands of the zeolite at 1990 and 1860 cm^{-1}.

The acidity of the external surface was measured by a gravimetric method using 2,6-di-*tert*-butylpyridine (DTBPy) as the probe molecule. Before adsorption, the sample in a U-type quartz tube was calcined at 550 °C in Ar for 4 h to remove physically absorbed water and air. Then it was cooled to 25 °C under Ar atmosphere protection and subsequently immersed in the DTBPy solution (predried by adding Na). After that, excess DTBPy was poured out rapidly, and physically adsorbed DTBPy was removed by calcining the sample in Ar at 250 °C for 12 h. The weight change of the sample after cooling to 25 °C was recorded by a high-accuracy magnetic suspension balance (Mettler-Toledo Al 104; sensitivity 0.1 mg). The density of external acid sites was calculated accordingly.

2.3. Surface Probe Reaction. The molecular size of 1,3,5-triisopropylbenzene (TIPB) is larger than the pore size of ZSM-5;[23] thus, its cracking occurs only on the external surface of the catalyst. The reaction was carried out at 350 °C under atmospheric pressure at a weight hourly space velocity (WHSV) of 0.5 h^{-1}.

OX is also unable to readily enter the pore of ZSM-5. Its transformation on the external surface of the catalyst was performed at 450 °C, atmospheric pressure, and a WHSV of 0.25 h^{-1} to determine the contributions from alkylation, isomerization, and dealkylation.

For comparison, PX was also used as the feedstock to study the transformation not only on the external surface but also inside the pores of the catalyst with the same operating conditions as when using OX as the feedstock. Conversion of OX or PX above was calculated on the basis of consideration of the residual OX or PX as the unreacted species, since we wanted to determine quantitatively the contribution of the isomerization of them.

2.4. Methanol-to-Aromatics Reaction. Two grams of catalyst was packed into the central zone of a fixed bed reactor of 12 mm i.d., and methanol (99.9% purity) mixed with N_2 in a volume ratio of 1:5 was preheated to 150 °C and fed into the reactor. Methanol was decomposed over the catalyst at 475 °C, atmospheric pressure, and a WHSV of methanol of 0.79 h^{-1}. The product, which included water, hydrocarbons, and hydrogen, was analyzed online with a gas chromatograph (Shimadzu, GC2014). The tubing between the reactor and GC was heated to 200 °C to prevent condensation of the products. Product selectivity and aromatics yield were calculated on a hydrocarbon basis. The selectivity was the average result in the first 1 h. Conversion of methanol was calculated on the basis of a consideration of the residual methanol and dimethyl ether as the unreacted species, considering the latter is very easily produced over a catalyst with very weak acids.

The reaction for 1 h at 475 °C resulted in coke deposition and deactivation of the catalyst. The methanol feed was switched off, and nitrogen was fed in to purge the residual organic compounds. Then air was fed into the reactor, and the coke was burned at 600 °C. The catalyst regeneration was considered completed when the total concentration of CO_2 and CO was lower than 0.05% in the off gas. Then the air feed was switched off, and nitrogen was fed in to purge the residual air to allow the feeding of methanol again. One reaction/catalyst-regeneration cycle needs 3 h in total. The reaction/catalyst-regeneration cycle was repeated six times to evaluate the stability of the catalyst.

DOI: 10.1021/acscatal.5b00192
ACS Catal. 2015, 5, 2982−2988

3. RESULT AND DISCUSSION

XRD characterization showed that the crystallinity of the ZSM-5 was decreased from 100% to 91.7% after the doping of Zn and P, and this was further decreased to 80% by the coating of the noncrystalline SiO_2 shell (Figure 1a). No peaks of Zn- and P-related species were found in the XRD pattern, suggesting Zn and P were monodispersed in the ZSM-5 framework. These were further validated by the TEM characterization (Figure S1 in the Supporting Information) that no obvious black particles were observed in the image. In addition, the Zn/P/ZSM-5 catalyst has a relatively well-defined crystal morphology, and it was changed into a round shape by a coating with a uniform but amorphous SiO_2 layer (Figure S1). Apparently, the amorphous SiO_2 shell resulted in a decrease in the crystallinity of the sample in XRD. A difference from previous works[21−25] was that the average thickness of the SiO_2 layer was only 32 nm, which did not change the average particle size of the catalyst significantly. In the thin SiO_2 shell, there is diffusion of reactants and products into and out from the ZSM-5 core, and it was this that gave the effect of increased PX selectivity.[14]

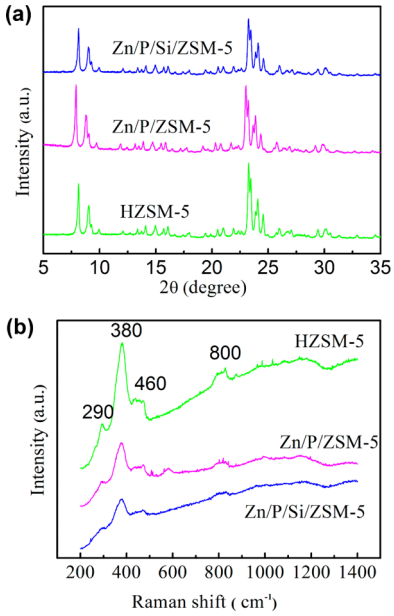

Figure 1. XRD pattern of different catalysts (a); Raman spectra of different catalysts (b). (a) and (b) both used the ZSM-5 with the Si/Al of 12.5.

The EDS results revealed that the Si/Al ratio on the edge of the sample was 32.2. This value is larger than that of Zn/P/ZSM-5 (17.7) and that of the pristine HZSM-5 (12.5; Figure S2 and Table S1). Because the external surface was completely coated with the SiO_2 layer, this value showed that the thin SiO_2 layer did not completely block the electron beam from detecting the Al species inside the core. Similarly, Raman characterization using a 432 nm laser showed that the peak intensity associated with the ZSM-5 crystal was significantly decreased by the doping of Zn and P and the coating with the SiO_2 shell (Figure 1b). In addition, the BET surface area of HZSM-5, Zn/P/ZSM-5 and Zn/P/Si/ZSM-5 were 402, 337, and 154 $m^2\ g^{-1}$, respectively (Table S2). The total pore volumes of these three catalysts were 0.251, 0.238, and 0.122 mL g^{-1}, respectively. The pore volumes of the micropores (<2 nm), mesopores (2−50 nm), and macropores (50−100 nm) decreased for Zn/P/Si/ZSM-5, as compared with those of Zn/P/ZSM-5(Table S2). These evidenced clearly that the SiO_2 shell resulted in the blocking of mesopores and macropores of the catalyst. However, the average pore size at 0.46−0.62 nm, which exhibited the shape-selective effect on PX, was nearly the same for the three catalysts (Table S2). Apparently, the SiO_2 shell of the catalyst exhibited a pore blocking effect slightly different from those in previous works.[14−21]

The distribution of the acid sites with different strengths on the three catalysts, determined by NH_3-TPD, is shown in Figure 2. The region above 400 °C was due to the desorption of NH_3 from strong Bronsted and Lewis acid sites.[26] The region below 400 °C in the NH_3-TPD was the contribution of the hydrogen bond form of the NH_4^+ cation[27,28] or was assigned to weak acid sites;[29−34] however, the continuous purging using He would exclude the first possibility.[26] In addition, this peak was also observed with a Zn/ZSM-5 catalyst used for several hundred hours but that still exhibited high activity.[13] Compared with HZSM-5, the doping of Zn and P resulted in the dealuminization of ZSM-5, in which the Si/Al ratio for Zn/P/ZSM-5 was 17.7 and 12.5 for pristine HZSM-5(Figure S2 and Table S1). Consequently, it resulted in a decrease in the amounts of acid centered at both 443 and at 228 °C, but increased the amount of acid centered at 342 °C. The doping with P replaced the strong bridged hydroxyl groups with a new type of acid site with a reduced acid strength.[35] In addition, the coating of Zn/P ZSM-5 by the SiO_2 shell reduced

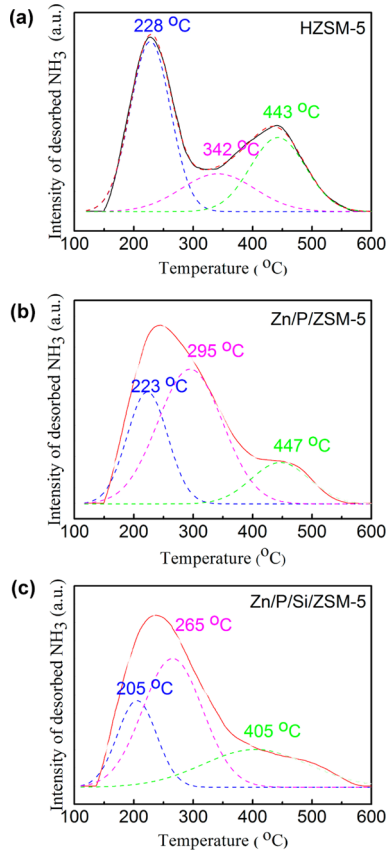

Figure 2. Acidity characterization of the three catalysts: NH_3-TPD profile of (a) HZSM-5, (b) Zn/P/ZSM-5, (c) Zn/P/Si/ZSM-5. Blue, pink, and green dashed lines in a, b, and c show the peaks obtained using Gaussian peak deconvolution.

DOI: 10.1021/acscatal.5b00192
ACS Catal. 2015, 5, 2982−2988

the amount of all types of acids by 1.9−12.6% (Figure 2c), if calculated on the basis of pure ZSM-5.[25,35−40]

The peak temperature of the medium strong and weak acid sites were shifted from 447 to 405 °C, from 295 to 265 °C, and from 228 to 205 °C, respectively. Similarly, in situ IR of adsorbed pyridine introduced the variation of the amount of total Lewis acid (centered at 1455 cm^{-1}) and total Bronsted acid (centered at 1545 cm^{-1}), measured after degassing at 200 °C, and medium strong Bronsted and Lewis acid (measured after degassing at 350 °C; Figure 3 and SI-3). The doping of Zn

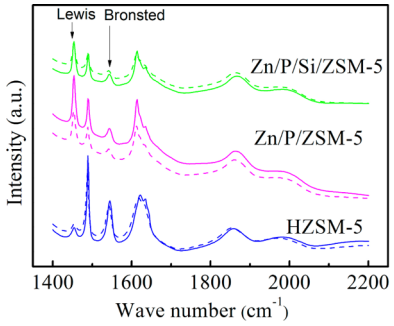

Figure 3. IR spectra of pyridine adsorption over the three catalysts (solid line for desorption at 200 °C and dashed line for desorption at 350 °C). The ZSM-5 used has a Si/Al ratio of 12.5.

and P resulted in both the amount of total Lewis acid and medium strong Lewis acid being increased while the amount of total Bronsted acid and strong Bronsted acid sites were reduced.[41−43] The coating of the SiO_2 shell on the catalyst decreased the amount of all types of acid sites by 23−38%, based on the total amount of catalyst (Table S3), or the acid amount, based on pure ZSM-5, was decreased by 15.9−26.6% (Table S4). The loss of Lewis acid sites was more significant than that of Bronsted acid sites because of the easy accessibility of Si species to the Lewis acid sites.[38] Quantitatively, the amount of external acid sites was probed by the adsorption of DTBPy, a large molecule that cannot enter the pores of the catalyst. The external acid sites accounted for 21.9%, 12.8% and 1.9% of the total amount of acid sites of HZSM-5, Zn/P/ZSM-5, and Zn/P/Si/ZSM-5 (Figure 4a), respectively. These results validated that the external acid sites were significantly suppressed by the coating of the SiO_2 shell.[20−25,35−40]

The catalytic performance in MTA of the three catalysts using ZSM-5 with a Si/Al ratio of 12.5 as the core was examined at 475 °C and atmospheric pressure (Figure 4b). Methanol conversions were all 100%, but the gross yields of aromatics were 44.65%, 76%, and 61.7% for HZSM-5, Zn/P/ZSM-5 and Zn/P/Si/ZSM-5, respectively. As compared with HZSM-5, the yield of aromatics over Zn/P/ZSM-5 was increased by 31.4% and the yield of liquefied petroleum gas (LPG, C_3−C_5) was decreased from 36.5% to 14.3%. The doping of Zn and P in ZSM-5 increased the amount of medium strong acid sites of ZSM-5, which enhanced the dehydrogenation and aromatization of LPG to aromatics.[13,42,44] The aromatic yield over Zn/P/Si/ZSM-5 was 14.3% lower than that over Zn/P/ZSM-5 because the coating with the SiO_2 layer reduced the amount of total acid sites of ZSM-5 by 7.02%. These comparisons validated that the strong acid sites in a large amount in the core of the catalyst are crucial for the aromatic yield. Meanwhile, the selectivity of PX over HZSM-5 and Zn/P/ZSM-5 was in the same range of 23.6−24.4%, although the

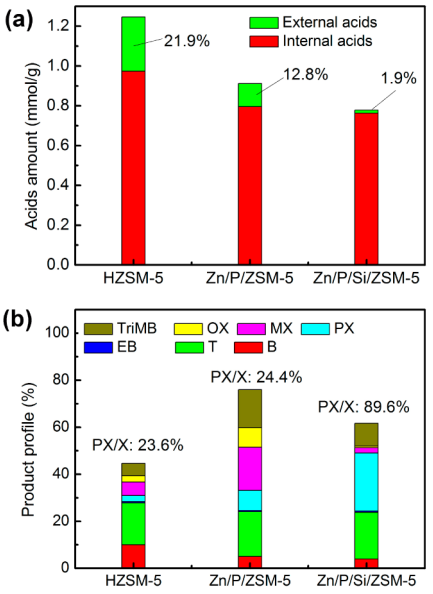

Figure 4. (a) External and internal acid amounts of the three catalysts. (b) Product profiles of MTA from the different catalysts. TriMB is trimethylbenzene.

external acid site amount was different. In sharp contrast, the selectivity of PX over Zn/P/Si/ZSM-5 was increased to 89.6% when the external acid sites were decreased to 1.9%. And the ratio of *meta*-X (MX) to PX decreased from 2.21 as over Zn/P/ZSM-5 to 0.082 as over Zn/P/Si/ZSM-5. These results clearly validated that the selectivity of PX was dominated by the amount of external acid sites, not by the total amount of acid sites of the catalyst. Thus, the structured ZSM-5 catalyst with the SiO_2 shell was crucial to meet the simultaneous requirement of high methanol conversion, total aromatic yield, and PX selectivity.

We further examined the effect of the Si/Al ratio of the ZSM-5 in the core on the catalytic performance (Figure 5). For Zn/P/ZSM-5, the increase in the Si/Al ratio of ZSM-5 from 12.5 to

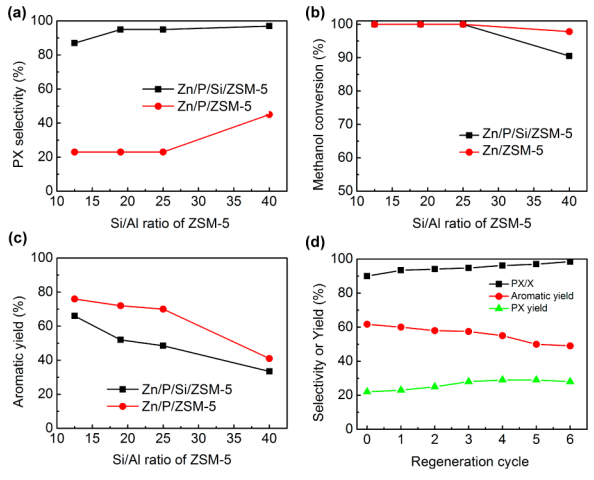

Figure 5. (a) Effect of ZSM-5 with different Si/Al ratios on the selectivity of PX. (b) Effect of ZSM-5 with different Si/Al ratios on the conversion of methanol. (c) Effect of ZSM-5 with different Si/Al ratios on the yield of aromatics. (d) Yield of aromatics, yield of PX, and selectivity of PX over Zn/P/Si/ZSM-5 in continuous reaction/catalyst-regeneration cycles. ZSM-5 used in part d had a Si/Al ratio of 12.5.

DOI: 10.1021/acscatal.5b00192
ACS Catal. 2015, 5, 2982−2988

25 did not increase the PX selectivity (Figure 5a) and did not influence the methanol conversion (Figure 5b), but resulted in a decrease in the acid amount, which resulted in a decrease in the aromatic yield (Figure 5c). Only when the Si/Al ratio of the ZSM-5 increased to 40 was the selectivity of PX increased from 23 to 24 to 42%, but both the methanol conversion and aromatics yield dropped drastically. In comparison, the coating with the SiO_2 shell on Zn/P/ZSM-5 allowed an increase in the PX selectivity to 89.6%, even when using as the core a ZSM-5 with a Si/Al of 12.5. It can be noted that a much higher PX selectivity could be obtained by the use of Zn/P/Si/ZSM-5 when the Si/Al ratio of the ZSM-5 core was high, but this was unable to achieve simultaneously a high conversion of methanol and a high aromatic yield. These comparisons validated that it is not a good choice to use ZSM-5 with relatively weak acid sites as the core, the external acid sites determine the isomerization of PX, and these were independent of the acidity at the core. In addition, both the acid strength and amount will be decreased at a higher temperature with some steam present (e.g., during catalyst regeneration).[13] In this case, the use of a ZSM-5 core with strong acid sites in a large amount is more favorable for maintaining the acidity for the catalyst to achieve a high regeneration stability. For instance, the catalyst with a ZSM-5 core with a Si/Al ratio of 12.5 exhibited good stability in producing aromatics in high yield and PX with high selectivity after six continuous reaction/catalyst-regeneration cycles (Figure 5d). In particular, the PX selectivity increase was sustainable with the regeneration cycle, indicating a surface change of the catalyst during regeneration.

The effect of weight ratio of SiO_2 shell on the PX selectivity, aromatic yield, and methanol conversion was also studied. The evolution of Si-containing species in the CLD process and calcinations has been well addressed previously.[23] Coating 8% SiO_2 on Zn/P/ZSM-5 resulted in a significant increase in the PX selectivity as compared with that of coating 5% SiO_2 (Figure 6a). Note that most of the external acids of the zeolite can be eliminated by increasing the CLD modification cycles.[23] Similarly, increasing the weight ratio of SiO_2 from 8% to 28% by the same way in the present work decreased the aromatic yield to some degree, but did not increase the PX selectivity significantly. In addition, one cycle modification as in the present work may result in the existence of residual silanol hydroxyls, which probably bring some acidic sites on the external surface. However, compared with other SiO_2-coated ZSM-5 catalysts used in other reactions,[21−25] the use of a much smaller amount of SiO_2 (8% of the catalyst) in the present work resulted in increasing PX selectivity effectively, while there was less influence on the other performance characteristics of the catalyst.

As follows, the surface probe reactions were used to understand the quantitative relationship between the external acid amount of the present catalyst on the PX selectivity or other reactions. First, TIPB, a large molecule that cannot enter the channel of ZSM-5, was cracked on the external surface of the catalyst (Figure S3). A water-free test conditions was used to ensure data accuracy. The conversion of TIPB decreased linearly with the amount of external acid sites in the range of 0.012−0.3 mmol g^{-1}, in agreement with a previous work.[24] However, there was no linear relationship between the amount of external acid sites with the PX selectivity in the MTA process (Figure 6b). The PX selectivity did not increase when the amount of external acid sites decreased from 0.012 to 0.06 mmol g^{-1}). Only when it was lower than 0.06 mmol g^{-1} did the

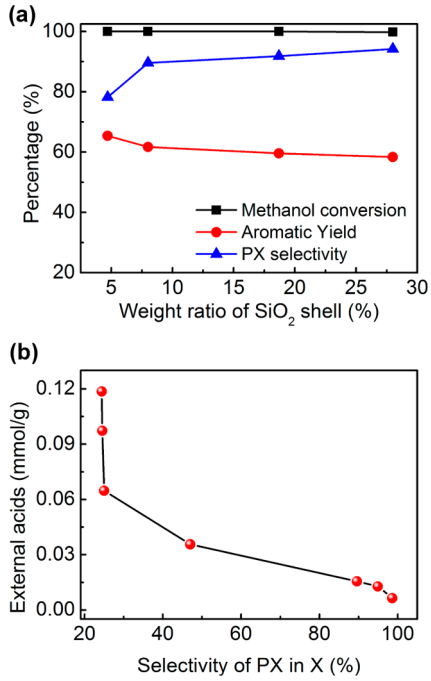

Figure 6. (a) Effect of weight ratio of SiO_2 shell on the PX selectivity, aromatic yield and methanol conversion. (b) Relationship between PX selectivity and amount of external acid sites.

PX selectivity begin to increase from 23% to 40%. When it decreased from 0.06 to 0.016 mmol g^{-1}, the PX selectivity increased drastically from 40% to 90%. It even approached 98.5% when the amount of external acid sites of the catalyst was 0.006 mmol g^{-1} (Figure 6b). These results validated that the selectivity of PX was directly related to the amount of external acid sites of the catalyst, and the isomerization of PX was more difficult to control compared with the cracking of TIPB. This evidence suggested that the ideal structure of a MTA catalyst should have a core with strong acid sites in a large amount and an external shell with weak acid sites in a small amount.

In addition, the effect of external acid sites of different catalysts on the dealkylation, isomerization, and alkylation was examined by the use of PX and OX as the feedstock at 475 °C (Figure 7a). The transformation of OX occurred mainly on the external surface of the catalyst because it cannot enter the pores of ZSM-5. In detail, the conversion of OX over Zn/P/ZSM-5 produced B, T, TriMB, EB, C_1−C_5 hydrocarbons, and mixed X with an equilibrium ratio, in which the selectivity of PX in X was 23%. The severe dealkylation of OX, isomerization of OX, and alkylation of OX above was attributed to the strong external acid sites in a large amount.[11] In sharp contrast, the conversion of OX over the external surface of Zn/P/Si/ZSM-5 was only 4.5%, in which the dealkylation of OX to B and T, alkylation of OX to TriMB, and the isomerization of OX to PX, MX, and EB contributed 1.1%, 0.4% and 3.1%, respectively. These results are evidence that the isomerization of X is more facile compared with alkylation or dealkylation on the external surface of the catalyst.[11,14]

The selectivity of OX over Zn/P/Si/ZSM-5 was 97%. In comparison, PX with a smaller molecular size enters the pores of ZSM-5 easily. Thus, the conversion of PX was much higher over Zn/P/ZSM-5, where it produced B, T, and TriMB, as compared with that of OX. Similarly, the conversion of PX was 76.1% over Zn/P/Si/ZSM-5 while maintaining a selectivity of

DOI: 10.1021/acscatal.5b00192
ACS Catal. 2015, 5, 2982−2988

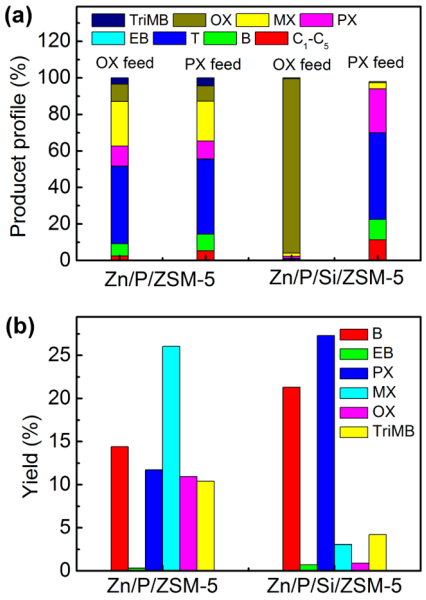

Figure 7. (a) Product distribution in the transformation of PX or OX over different catalysts. EB is ethylbenzene. (b) Product distribution of the alkylation of methanol and T over different catalysts.

PX of 85.8%. If there is the same activity of PX as OX on the external surface of Zn/P/Si/ZSM-5, we can determine that 4.5% of PX was transformed on the external surface and 71.6% of PX was transformed inside the pores into other aromatics. Strikingly, the strong acidity at the core of this catalyst resulted in the severe dealkylation of PX to B and T, which contributed 59.8% in total 71.6% transformation of PX inside the pores. The result also explained well the wide production profile of B, T, X, and TriMB in the MTA reaction (Figure 4b). However, the weight ratio of B plus T was 39% in the MTA reaction, which is less than that (58.6%) in the transformation of PX above. Possibly, the presence of methanol produced side-on or end-on adsorbed complexes on the external surface of ZSM-5[45] and suppressed the dealkylation of the produced X. The carbocation intermediate will be more stable with more methyl groups on the aromatic ring.

In addition, the methylation rate constant over HZSM-5 decreased from T to X, which resulted from the change in the dominant surface species prior to the rate-determining step.[46] The unusual decrease in the methylation rate constant was ascribed to a diffusion limitation for X and larger aromatics in the ZSM-5 channel.[47] For methanol conversion over HZSM-5, Zn/P/ZSM-5, and Zn/P/Si/ZSM-5 in the present work (Figure 4b), the weight ratio of total X to T in the product is 0.65, 1.88, and 1.43, respectively. The weight ratio of total X to TriMB is 2.17, 2.21, and 2.90, respectively, and the weight ratio of TriMB to T is 0.30, 0.85, and 0.49, respectively. These comparisons indicated that X is a dominant product over Zn/P/ZSM-5 and Zn/P/Si/ZSM-5, in agreement with the conclusion that methylation of T is quicker than methylation of X,[46] and the amount of TriMB will be suppressed due to its low diffusion rate.[47]

In addition, the alkylation of methanol and T with the weight ratio of 2:1 was tested over Zn/P/Si/ZSM-5(Figure 7b). A high methanol conversion (>95%), high yield of aromatics (>60%), and high selectivity of PX were simultaneously obtained. The PX selectivity was 83.7% at 15 min and 94% at 30 min. This may be because the deposition of coke in a small amount narrowed the pore size and covered the acid site of the zeolite,[17,25,35−37,47−49] resulting in the increase in the PX selectivity. A similar trend was found in the MTA reaction with prolonged reaction time, in which the selectivity of PX in X increased only from 85.8% to 90%. Because the PX selectivity in the fresh Zn/P/Si catalyst was higher than 85%, we concluded that the contribution of coke deposition to the increase in the PX selectivity was less compared with the effect of coating a SiO_2 shell on the catalyst. On the other hand, the result above also validated that it is possible to recycle B and T to produce PX in high yield in the MTA process. All these results confirmed that the weak external acid sites in a small amount played the important role of suppressing isomerization, alkylation, and dealkylation to achieve a high selectivity of PX. In this case, a high yield of PX can be achieved in the MTA process over Zn/P/Si/ZSM-5 by a single pass conversion of methanol and the recycled conversion of B and T with methanol.

4. CONCLUSION

By coating a 8% SiO_2 layer on a Zn/P/ZSM-5 catalyst, we were able to decrease the external acidity of the catalyst having a core with strong acid sites in a large amount. We validated that the core of ZSM-5 with strong acid sites in a large amount was crucial for a high methanol conversion and high yield of aromatics. The outer shell of SiO_2 with weak acid sites in a small amount played an important role in increasing the selectivity of PX in X. A 61.7% yield of aromatics, nearly 100% conversion of methanol, and 89.6% selectivity of PX were simultaneously achieved, and the catalyst exhibited good stability in continuous reaction/catalyst-regeneration cycles. The catalyst was also active in converting recycled T into PX by the alkylation of methanol and T. This allowed the achievement of a high PX yield in a single pass conversion of methanol in the MTA reaction and allowed the simplification of the separation of PX from its isomers.

■ ASSOCIATED CONTENT

Supporting Information

The following file is available free of charge on the ACS Publications website at DOI: 10.1021/acscatal.5b00192.

TEM characterization, EDS result, BET surface area, pore volume distribution of different catalysts and the relationship between the conversion of TIPB and the external acid amount (PDF)

■ AUTHOR INFORMATION

Corresponding Author

*Fax: +86 10 6277 2051. E-mail: qianwz@tsinghua.edu.cn.

Notes

The authors declare no competing financial interest.

■ ACKNOWLEDGMENTS

We are grateful for support from NSFC program of 21376135, 91434122, and 51236004. We are also grateful to Prof. D. Z. Wang for discussions on the reaction mechanism.

■ REFERENCES

(1) Ilias, S.; Bhan, A. *ACS Catal.* **2012**, *3*, 18−31.
(2) Olsbye, U.; Svelle, S.; Bjorgen, M.; Beato, P.; Janssens, T. V. W.; Joensen, F.; Bordiga, S.; Lillerud, K. P. *Angew. Chem., Int. Ed.* **2012**, *51*, 5810−5812.

DOI: 10.1021/acscatal.5b00192
ACS Catal. 2015, 5, 2982−2988

(3) Shen, K.; Wang, N.; Cui, Y.; Qian, W. Z.; Wei, F. *Catal. Sci. Technol.* **2014**, *4*, 3840−3844.
(4) Shen, K.; Qian, W. Z.; Wang, N.; Su, C.; Wei, F. *J. Am. Chem. Soc.* **2013**, *135*, 15322−15325.
(5) Shen, K.; Qian, W. Z.; Wang, N.; Zhang, J. G.; Wei, F. *J. Mater. Chem. A* **2013**, *1*, 3272−3275.
(6) Inoue, Y.; Nakashiro, K.; Ono, Y. *Microporous Mater.* **1995**, *4*, 379−383.
(7) Song, Y. Q.; Zhu, X. X.; Xu, L. Y. *Catal. Commun.* **2006**, *7*, 218−223.
(8) Lopez-Sanchez, J. A.; Conte, M.; Landon, P.; Zhou, W.; Barley, J. K.; Talyor, S. H.; Carley, A. F.; Kiely, C. J.; Khali, K.; Hutchings, G. J. *Catal. Lett.* **2012**, *142*, 1049−1056.
(9) Zaidi, H. A.; Pant, K. K. *Catal. Today* **2004**, *96*, 155−160.
(10) Freeman, D.; Wells, R. P. K.; Hutchings, G. J. *J. Catal.* **2002**, *205*, 358−365.
(11) Zhang, J. G.; Qian, W. Z.; Tang, X. P.; Shen, K.; Wang, T.; Huang, X. F.; Wei, F. *Acta. Phys. Chim. Sin.* **2013**, *29*, 1281−1288.
(12) Keil, F. J. *Microporous Mesoporous Mater.* **1999**, *29*, 49−66.
(13) Wang, T.; Tang, X. P.; Huang, X. F.; Qian, W. Z.; Cui, Y.; Hui, X. Y.; Yang, W.; Wei, F. *Catal. Today* **2014**, *233*, 8−13.
(14) Ahn, J. H.; Kolvenbach, R.; Al-Khattaf, S. S.; Jentys, A.; Lercher, J. A. *Chem. Commun.* **2013**, *49*, 10584−10586.
(15) Young, L. B.; Butter, S. A.; Kaeding, W. W. *J. Catal.* **1982**, *76*, 418−432.
(16) Mirth, G.; Cejka, J.; Lercher, J. A. *J. Catal.* **1993**, *139*, 24−33.
(17) Kaeding, W. W.; Chu, C.; Young, L. B.; Weinstein, B.; Butter, S. A. *J. Catal.* **1981**, *67*, 159−174.
(18) Kim, J. H.; Namba, S.; Yashima, T. *Appl. Catal., A* **1992**, *83*, 51−58.
(19) Ivanova, I. I.; Corma, A. *J. Phys. Chem. B* **1997**, *101*, 547−551.
(20) Zheng, S. R.; Heydenrych, H. R.; Roger, H. P.; Jentys, A.; Lercher, J. A. *Top. Catal.* **2003**, *22*, 101−106.
(21) Wang, I.; Ay, C. L.; Lee, B. J.; Chen, M. H. *Appl. Catal.* **1989**, *54*, 257−266.
(22) Weber, R. W.; M?ller, K. P.; Unger, M.; O'Connor, C. T. *Microporous Mesoporous Mater.* **1998**, *23*, 179−187.
(23) Zhu, Z. R.; Xie, Z. K.; Chen, Q. L.; Kong, D. J.; Li, W.; Yang, W. M.; Li, C. *Microporous Mesoporous Mater.* **2007**, *101*, 169−175.
(24) Inagaki, S.; Shinoda, S.; Kaneko, Y.; Takechi, K.; Komatsu, R.; Tsuboi, Y.; Yamazaki, H.; Kondo, J. N.; Kubota, Y. *ACS Catal.* **2013**, *3*, 74−78.
(25) Niwa, M.; Kato, M.; Hattori, T.; Murakami, Y. *J. Phys. Chem.* **1986**, *90*, 6233−6237.
(26) Ferenc, L.; Jozsef, V. *Microporous Mesoporous Mater.* **2001**, *47*, 293−301.
(27) Barthos, R.; Lonyi, F.; Onyestyak, G.; Valyon, J. *J. Phys. Chem. B* **2000**, *104*, 7311−7319.
(28) Katada, N.; Igi, H.; Kim, J. H.; Niwa, M. *J. Phys. Chem. B* **1997**, *101*, 5969−5977.
(29) Tan, W.; Liu, M.; Zhao, Y.; Hou, K. K.; Wu, H. Y.; Zhang, A. F.; Liu, H. O.; Wang, Y. R.; Song, C. S.; Guo, X. W. *Microporous Mesoporous Mater.* **2014**, *196*, 18−30.
(30) Meshram, N. R.; Hegde, S. G.; Kulkarni, S. B. *Zeolites* **1986**, *6*, 434−438.
(31) Woolery, G. L.; Kuehl, G. H.; Timken, H. C.; Chester, A. W.; Vartuli, J. C. *Zeolites* **1997**, *19*, 288−296.
(32) Karge, H. G.; Dondur, V. *J. Phys. Chem.* **1990**, *94*, 765−772.
(33) Lok, B. M.; Marcus, B. K.; Angell, C. L. *Zeolites* **1986**, *6*, 185−194.
(34) Topsoe, N. Y.; Pedersen, K.; Derouane, E. G. *J. Catal.* **1981**, *70*, 41−52.
(35) Kim, J. H.; Ishida, A.; Okajima, M.; Niwa, M. *J. Catal.* **1996**, *161*, 387−392.
(36) Kim, J. H.; Kunieda, T.; Niwa, M. *J. Catal.* **1998**, *173*, 433−439.
(37) Hibino, T.; Niwa, M.; Murakami, Y. *J. Catal.* **1991**, *128*, 551−558.
(38) Zheng, S. R.; Heydenrych, H. R.; Jentys, A.; Lercher, J. A. *J. Phys. Chem. B* **2002**, *106*, 9552−9558.
(39) Fraenkel, D. *Ind. Eng. Chem. Res.* **1990**, *29*, 1814−1821.
(40) Fang, L. Y.; Liu, S. B.; Wang, I. *J. Catal.* **1999**, *185*, 33−42.
(41) El-Malki, E. M.; Van Santen, R. A.; Sachtler, W. M. H. *J. Phys. Chem. B* **1999**, *103*, 4611−4622.
(42) Biscardi, J. A.; Meitzner, G. D.; Iglesia, E. *J. Catal.* **1998**, *179*, 192−202.
(43) Xue, N. H.; Chen, X. K.; Nie, L.; Guo, X. F.; Ding, W. P.; Chen, Y.; Gu, M.; Xie, Z. K. *J. Catal.* **2007**, *248*, 20−28.
(44) Choudhary, V. R.; Panjala, D.; Banerjee, S. *Appl. Catal., A* **2002**, *231*, 243−251.
(45) Forester, T. R.; Howe, R. F. *J. Am. Chem. Soc.* **1987**, *109*, 5076−5082.
(46) Hill, I. M.; Malek, A.; Bhan, A. *ACS Catal.* **2013**, *3*, 1992−2001.
(47) Ahn, J. H.; Kolvenbach, R.; Al-Khattaf, S. S.; Jentys, A.; Lercher, J. A. *ACS Catal.* **2013**, *3*, 817−825.
(48) Mores, D.; Stavitski, E.; Kox, M. H.F.; Kornatowshi, J.; Olsbye, U.; Weckhuysen, B. M. *Chem. - Eur. J.* **2008**, *14*, 11320−11327.
(49) Cejka, J.; Zilkova, N.; Wichterlova, B.; Eder-Mirth, G.; Lercher, J. A. *Zeolites* **1996**, *17*, 265−271.

DOI: 10.1021/acscatal.5b00192
ACS Catal. 2015, 5, 2982−2988